RSC Applied Polymers

ROYAL SOCIETY OF CHEMISTRY

PAPER

View Article Online
View Journal | View Issue

Cite this: *RSC Appl. Polym.*, 2025, **3**, 875

Development of casein-based nanonutraceuticals by entrapping anthocyanin derived from secondary-agricultural residues: a step towards functional food additives†

Maninder Meenu,*[a] Mansi,‡[b] Anil Kumar Pujari,‡[b] Monika Garg *[a] and Jayeeta Bhaumik*[b]

This study aims to extract anthocyanins (ACNs) from different secondary-agricultural residues and encapsulate them using casein to enhance their stability and bioavailability. Ultrasonic-assisted and conventional extraction methods yielded substantial anthocyanin content from black plum (BP), blueberry (BB), and black wheat bran (WB). After purification, ACNs were encapsulated with casein through the desolvation technique. The optimized anthocyanin-casein-based nanoparticles (A-CNPs) resulted in satisfactory size, polydispersity index (PDI), and zeta potential values of 196–201 nm, 0.184–0.241, and −36 to −34 mV, respectively. BB@A-CNPs resulted in the highest encapsulation efficiency of 92% compared to BP@A-CNPs (83%) and WB@A-CNPs (72%). BP@A-CNPs, WB@A-CNPs, and BB@A-CNPs exhibited high storage stability for 28 days. A-CNPs, particularly BB@A-CNPs, exhibited improved stability towards temperature, pH change, and light. Furthermore, the gastrointestinal stability and release of ACNs from BB@A-CNPs were also assessed using an *in vitro* digestion model. The controlled release of ACNs and the high antioxidant activity of the final digest suggest improved bioavailability of BB@A-CNPs. Thus, BB@A-CNPs can be used as functional food additives for potentially enriching dairy products with health-promoting anthocyanins. These findings support further development and *in vivo* validation of the application of these nanonutraceuticals as food additives.

Received 7th December 2024,
Accepted 30th April 2025

DOI: 10.1039/d4lp00363b

rsc.li/rscapplpolym

1. Introduction

Anthocyanins (ACNs) are water-soluble pigments found in plants, belonging to the flavonoid class within the polyphenolic group. ACNs are widely present in nature and impart different colors to various plant parts.[1] ACNs have a C6–C3–C6 skeletal structure and are considered ideal natural colorants. These natural pigments provide various health benefits such as anticancer, antioxidant, antimicrobial, and anti-inflammatory effects.[2] Recently, ACNs have been widely used in the food, cosmetics, and pharmaceutical industries as functional ingredients. ACNs are used as food colorants in food products such as pancakes, omelettes, milkshakes, fermented milk, cream cheese, and low-pH beverages.[3,4]

Secondary-agricultural residues such as black wheat bran (WB), low-grade black plum (BP), and blueberry (BB) have been reported as rich and economical sources of ACNs.[5] ACN extraction from secondary-agricultural residues using green solvents results in safe and cost-effective ACNs, which can be used as natural colorants or functional additives in foods.[2,5]

However, the application of ACNs in the food industry is limited due to their molecular instability towards pH, temperature, and light.[6] In addition, ACNs also exhibit poor bioavailability due to their degradation during gastrointestinal digestion. Therefore, innovative technological strategies are required to improve the stability of ACNs. Encapsulation is described as a process of entrapping polyphenols, including ACNs, using natural polymers as wall materials to enhance the efficiency of bioactive compounds by improving their solubility, stability, and bioavailability.[3,7] The size of encapsulated particles can be classified as nano (<1 μm), micro (1–5000 μm), and macro (>5000 μm).[8–10] Nanoencapsulation of ACNs in biopolymeric nanostructures has been demonstrated

[a]*Division of Agricultural Biotechnology, National Agri-Food Biotechnology Institute (NABI), Sector 81, Sahibzada Ajit Singh Nagar, Punjab-140308, India. E-mail: meenu_maninder@yahoo.com, mkajgarg@gmail.com; Tel: +91 75895 92370, +91 172 522 1205*

[b]*Department of Nanomaterial and Application Technology, Center of Innovative and Applied Bioprocessing (CIAB), Sector 81, Sahibzada Ajit Singh Nagar, Punjab-140308, India. E-mail: jayeeta@ciab.res.in; Tel: +91 172 5221539*

†Electronic supplementary information (ESI) available: Supplementary file. See DOI: https://doi.org/10.1039/d4lp00363b

‡Equal contribution.

to be a successful strategy to enhance the stability and bioavailability of ACNs owing to their smaller size.[11]

Several researchers have developed protein-based nanoparticle delivery systems to encapsulate, protect, and transport ACNs to the target system. For instance, studies have reported enhanced antioxidant activity, as well as improved thermal and gastrointestinal stability when red raspberry pomace ACNs were loaded onto β-lactoglobulin nanoparticles compared to free molecules.[3] The nanoencapsulation of ACNs using amphiphilic peptides retained the free radical scavenging activity of ACNs (cyanidin 3-*O*-glucoside) and improved ACN stability towards pH and temperature.[1] Furthermore, evidence indicated that nanoencapsulation of blackberry ACNs using pectin and lysozyme self-assembly leads to the excellent physical stability of ACNs in different pH ranges.[6] The nanoencapsulation of mulberry ACNs using sodium caseinate-konjac glucomannan nanoparticles was also reported to enhance the stability and bioavailability of ACNs.[12]

Thus, the present study is directed towards the development of green and cost-effective casein-based nanonutraceuticals using ACNs extracted from secondary-agricultural residues such as black wheat bran (WB), low-grade black plum (BP), and blueberry (BB). ACNs were nanoencapsulated with casein by employing a simple desolvation technique. The resultant casein-based ACN nanoparticles (A-CNPs) were characterised by employing various analytical techniques. Furthermore, the stability of the synthesised A-CNPS was evaluated over 28 days of storage at room temperature, as well as towards pH, temperature, and gastrointestinal digestion. These resultant nanonutraceuticals entrapped with ACNs (A-CNPs) can further be used as additives in flavoured water and ultra-high treated beverages.

2. Materials and methods

2.1. Chemicals

The analytical grade (AR) chemicals used in this study were procured from Sisco Research Laboratories Pvt. Ltd (SRL), Mumbai, and Central Drug House (P) Ltd, CDH, New Delhi, India. Casein from bovine milk was purchased from Sigma-Aldrich Chemicals Private Limited, India. Ultrapure water was collected from a Direct-Q® 3 UV water purification system from Merck Millipore, Mumbai, India.

2.2. Raw material for anthocyanin

Black wheat (NABI MG-11) is grown in NABI, Mohali, Keylong, Himachal Pradesh, and other cities of India. Black wheat bran (WB) is a by-product of bakery experiments conducted at NABI Mohali, India.[13,14] During the fruiting season, significant fruit drops are collected under the tree and discarded as waste. Thus, these overripe fruit drops of black plum (BP) were collected from the horticultural lands of NIPER Mohali, India. Blueberry (BB) is an expensive and exotic fruit with a limited shelf life. Vendors usually discard unsold, low-grade BB as waste. Thus, these low-grade shrivelled BB were collected from a local fruit market in Chandigarh, India. Sample collection was done in 2023. BP and BB were cleaned to remove bruised fruits and foreign materials, followed by washing under running tap water and air-drying. BP was deseeded and then BP and BB were processed in a blender to make a paste. All these samples were stored in air-tight food-grade containers at −80 °C until further analysis.

2.3. Anthocyanin extraction and purification

ACN extraction and purification were conducted according to previously reported methods optimized in our laboratory.[5] ACNs from WB were extracted by employing the conventional shaking method. The ball-milled wheat bran sample (100 g) was extracted with 1 L acidic water (1% HCl) for 18 hours at 28 °C. After centrifugation, the pellet was again extracted with 1 L of solvent for 5 h, followed by centrifugation. Both supernatants were combined and kept at −20 °C for the precipitation of heavier molecules. Then, the clear supernatant was obtained by centrifugation, preconcentrated with reverse osmosis, and lyophilized.

ACNs from BP and BB were extracted by the ultrasonic-assisted extraction (UAE) method. Briefly, samples (100 g) were mixed with 1 L acidic aqueous ethanol (72.5% EtOH and 0.02% HCl v/v), followed by UAE twice for 30 min at 40 kHz and 480 W using a Branson 2800 ultrasonicator (M2800H-E, Danbury, USA). The mixture was centrifuged, and both supernatants were combined, kept at −20 °C overnight, and then centrifuged and lyophilized.

Furthermore, lyophilized ACN extracts were purified by employing ion exchange chromatography using Amberlite XAD-7 as resin. The purified ACNs were concentrated using a rotary evaporator and then lyophilized and stored at −80 °C.

2.4. Determination of anthocyanin content

The ACN content of samples was determined using the pH differential method.[15] The samples were four times diluted with 25 mM potassium chloride buffer (pH 1.0) and 0.4 M sodium acetate buffer (pH 4.5), and the absorbance was recorded at 520 and 700 nm. The anthocyanin content (mg L^{-1}) was expressed as cyanidin-3-*O*-glucoside (C3G) equivalents according to the following equation:

$$\text{Anthocyanin content}\,(\text{mg L}^{-1}) = \frac{(\Delta A \times \text{MW} \times \text{DF} \times 1000)}{\varepsilon \times 1} \quad (1)$$

where $\Delta A = A_{520\ \text{nm}} - A_{700\ \text{nm}}$; M_w = molecular weight of C3G (449.2 g mol^{-1}); DF = dilution factor; ε = molar extinction coefficient of C3G (26 900 mol L^{-1} cm^{-1}); 1 = path length of the cuvette in cm.

2.5. Determination of individual anthocyanins by LC-MS/MS

The LC-MS/MS analysis was performed according to a previously established method[16] for the identification of individual anthocyanins. Briefly, lyophilized anthocyanin extracts (1 mg) were dissolved in 10 mL of acidic water (0.1% trifluoroa-

cetic acid, TFA) to prepare the sample solution. The resulting solution was filtered through a 0.22 μm polytetrafluoroethylene (PTFE) filter to ensure the removal of particulate matter. Analyses were conducted using a Waters UPLC system coupled with an AB Triple TOF 5600 Plus mass spectrometer (AB SCIEX, Framingham, MA, USA), operating in a scan range of 50–1000 m/z.

2.6. Nanoencapsulation of purified anthocyanins using casein (A-CNPs)

Casein-based nanoparticles were synthesized using the desolvation technique. Briefly, 100 mg of casein was dissolved in 10 mL of ultrapure water (pH 9). The solution was stirred for 8 h at 500 rpm using a magnetic stirrer for complete hydration. Then, purified ACN (1 mg) at pH 5 was added to the casein solution at a rate of 1 mL min^{-1} under sonication. Then, 0.1 ml of 4% calcium chloride–ethanol solution was added for intra-particle cross-linking, followed by 45 min of sonication. The casein : ACN ratio (100 : 1 w/w) was optimised based on DLS data of different casein : ACN ratios (100 : 1, 100 : 3, 100 : 5 and 100 : 10 w/w). Empty CNPs were also formed using the same method without adding ACN. For further characterization, the solution was centrifuged for 20 min at 15 000g at 4 °C. The pellet of nanoparticles was resuspended in water and stored at 4 °C till further analysis.[17]

2.7. Characterization of anthocyanin-encapsulated casein nanoparticles (A-CNPs)

2.7.1. Dynamic light scattering (DLS) analysis. The size, PDI, and zeta potential of bare CNP and A-CNP samples were analyzed by using the DLS method (Zetasizer particle analyzer, Malvern) with a fixed angle detector of 173° at 25 °C. For this, a stock solution of bare CNPs and A-CNPs (1 mg mL^{-1}) was prepared in water. This stock solution was transferred to a disposable cuvette and analyzed for size, PDI, and zeta potential.[6]

2.7.2. Encapsulation efficiency (EE). The EE of A-CNPs was determined according to a previously described method.[11] Briefly, the synthesized A-CNPs were centrifuged for 20 min at 15 000g to collect the pellet of A-CNPs. The free ACN content in a clarified supernatant was determined by employing the pH differential method as mentioned in section 2.4 using the following equation:

$$\mathrm{EE}(\%) = \frac{\text{Total anthocyanins-Free anthocyanins}}{\text{Total anthocyanins}} \times 100 \quad (2)$$

2.7.3. Scanning electron microscopy (SEM) and transmission electron microscopy (TEM) analysis. The bare CNP and A-CNP samples were drop-cast on a silicon wafer and air-dried overnight at room temperature. Then, the samples were gold-coated for 2 min with an ion sputter system (Q150T ES Quorum, UK) and observed under an SEM (Model No.1142265, Thermo Fisher Scientific, Czech Republic) at 10 kV.

2.7.4. Fourier-transform infrared (FTIR) spectroscopy. The FTIR spectra of casein, purified ACNs, and lyophilized A-CNPs were acquired using an FT-IR spectrometer (PerkinElmer UATR Two, USA) equipped with an attenuated total reflectance (ATR) accessory. The sample was placed on a diamond crystal, and spectra were collected from 4000 to 400 cm^{-1} with a spectral resolution of 4 cm^{-1} while keeping the sample in contact with the diamond crystal.

2.7.5. HPLC analysis. HPLC analyses of the nanoformulations were performed to evaluate the anthocyanin content,[30] using 0.4% TFA in acetonitrile : water (9 : 1) and a run time of 30 min.

2.8. Stability study of casein-encapsulated anthocyanin nanoparticles

The stability studies of the synthesized A-CNPs were conducted using previously described methods[1,12] as explained below.

2.8.1. Storage stability. For the stability study, bare CNP and A-CNP samples were stored in 15 mL Falcon centrifuge tubes at room temperature for 28 days, and the DLS data of A-CNPs were collected at an interval of one week as mentioned in section 2.6.1.

2.8.2. Thermal stability. The purified ACNs and A-CNPs were heated at 80 °C for 5 h. After cooling down samples to room temperature, the retention rate of ACNs following thermal treatment was estimated using the pH differential method and the following equation, as mentioned in the literature.[12]

$$\text{Anthocyanin retention rate}(\%) = \frac{\text{Final anthocyanin content}}{\text{Total anthocyanin content}} \times 100 \quad (3)$$

2.8.3. pH stability. The purified ACNs and A-CNPs were mixed with 1 M HCl and 1 N NaOH to achieve pH values of 1.0, 4.0, 6.0, 7.0, and 9.0. After mixing, the samples were kept in the dark for 6 h at 4 °C. The retention rate of ACNs was then determined using the pH differential method, employing eqn (1) and (3).[1]

2.8.4. Light stability. The purified ACNs and A-CNPs were stored in Falcon centrifuge tubes at room temperature and exposed to light for 16 h for 28 days under laboratory conditions. These conditions were used to mimic the environment of regional supermarkets. After four weeks, the ACN retention rate was determined using the pH difference method by employing eqn (1) and (3).[12]

2.9. Simulated gastrointestinal digestion

The A-CNPs were subjected to simulated gastrointestinal digestion for the release of ACNs from casein nanoparticles. Briefly, a 10 mL sample was mixed with 5 mL of simulated oral fluid composed of 0.2% α-amylase in phosphate-buffered saline (pH 6.8). This mixture was incubated at 37 °C and 100 rpm for 5 min. The resultant oral digestive fluid was mixed with 15 mL of simulated gastric juice (SGJ) composed of 3 g L^{-1} pepsin and 9 g L^{-1} saline (pH = 3). This mixture was again incubated at 37 °C for 2 h. After gastric digestion, the resultant fluid was subjected to intestinal digestion in 15 mL of simulated intesti-

nal juice (SIJ) composed of 3 g L^{-1} of bile salt and 10 g L^{-1} pancreatic enzyme in phosphate buffered solution (pH = 8). This mixture was again incubated in a temperature-controlled shaker. During the whole digestion (4 h), 2 mL samples were taken after fixed intervals of time and kept at −20 °C for further use.[18,19] The amount of ACN released after a particular digestion interval was calculated based on the pH differential method as mentioned in section 2.4. The antioxidant potential of purified BB ACN and BB@A-CNPs before gastrointestinal digestion (BD) and after gastrointestinal digestion (AD) was determined by employing DPPH and ABTS assays as mentioned previously.[5] For the ABTS assay, 7 mM ABTS solution was mixed with 2.45 mM potassium persulphate (1 : 1, v/v) and incubated for 12 h at room temperature to prepare ABTS free radical solution. Then 140 mL of the ABTS free radical solution was added to 850 mL of the sample, followed by vigorous shaking. After 15 min of incubation at room temperature, the absorbance of the reaction mixture was observed at 734 nm. The percentage scavenging activity of ABTS free radicals by A-CNPs was calculated using the following equation:

$$\text{ABTS scavenging activity}(\%) = (\text{Abs}_{\text{control}} - \text{Abs}_{\text{sample}})/\text{Abs}_{\text{control}} \times 100 \quad (4)$$

where $\text{Abs}_{\text{control}}$ is the absorbance of ABTS cation radical solution and $\text{Abs}_{\text{sample}}$ is the absorbance of ABTS cation radical solution after reaction with the sample.

For the DPPH assay, DPPH solution (0.14 mM) was prepared in methanol. Then, 850 mL of sample was mixed with 140 mL of DPPH solution, followed by vigorous shaking. After 30 min of incubation in the dark, the absorbance of the reaction mixture was recorded at 517 nm. The percentage scavenging activity of DPPH free radicals by the sample was calculated using the following equation:

$$\text{DPPH scavenging activity}(\%) = (\text{Abs}_{\text{control}} - \text{Abs}_{\text{sample}})/\text{Abs}_{\text{control}} \times 100 \quad (5)$$

where $\text{Abs}_{\text{control}}$ is the absorbance of only the DPPH solution and $\text{Abs}_{\text{sample}}$ is the absorbance of the DPPH cation radical after reaction with the sample.

2.10. Statistical analysis

Each experiment was conducted thrice, and data were presented as mean ± standard deviation. Statistical analysis was conducted by employing one-way ANOVA using SPSS version 19 (IBM, USA). The graphs were plotted using Origin 2021 software (OriginLab Co. Ltd, USA). $p \leq 0.05$ indicated significant differences among the mean values of different samples.

3. Results and discussion

3.1. Anthocyanin extraction and purification

Black WB, overripe fruit drops of BP, and shrivelled BB contain significant amounts of ACNs. The TAC in BB, WB, and BP was 341.46 ± 3.18 mg L^{-1} (wet basis), 325.83 ± 5.51 mg L^{-1} (dry basis), and 59.72 ± 1.83 mg L^{-1} (wet basis), as mentioned in ESI Fig. 1.† In the literature, significant variations in the TAC values of BB and BP have been reported.[20,21] These variations are attributed to the differences in varieties, geographical regions, environmental conditions, and ripening stages of fruits.[20–22] These crude ACN extracts were further purified to remove any protein and hydrocolloid present. The weight of the resultant semi-pure extracts was reduced by 68.91%, 41.31%, and 41.79% compared to BP, WB, and BB crude extracts, respectively. These resultant semi-pure extracts were further purified using ion exchange chromatography using Amberlite XAD-7 resin. The subsequent purified ACN extracts were reduced to 94.67%, 91.24%, and 95.67% of the semi-pure ACN extracts of BP, WB, and BB, respectively. These findings were in accord with a previous study focused on extracting and purifying ACNs from edible flowers.[23] Similar findings were also reported in our previous study focused on the extraction of anthocyanins from WB, BB, and BP, followed by their application in the development of bionanocomposite packaging films.[5]

3.2. Nanonutraceutical preparation by encapsulation of purified anthocyanins into casein

After adjusting the pH, purified ACNs were encapsulated using casein, as shown in Scheme 1. Initially, the casein to ACN ratio (100 : 1, 100 : 3, 100 : 5, and 100 : 10 w/w) was optimized based on the DLS data (size, PDI, and zeta potential) of the synthesized A-CNPs.

During the nanoencapsulation of active materials, smaller nanoparticles are preferred due to their greater stability, resistance to precipitation, and enhanced functionality.[24] Studies have also shown that increasing the quantity of either the wall or the core material leads to larger nanoparticle sizes. Therefore, optimizing the proportions of wall and core materials is crucial for synthesizing highly stable nanoparticles with minimal size.[24,25] As mentioned in Table 1, the particle sizes of BP@A-CNPs, WB@A-CNPs, and BB@A-CNPs ranged from 198.17–228.97, 196.73–249.67, and 201.10–368.63 nm, with different concentrations of ACNs, respectively. Meanwhile, the PDI values varied from 0.219–0.462,

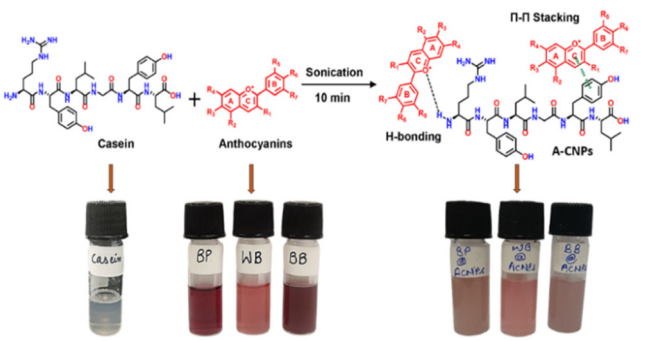

Scheme 1 Schematic presentation the synthesis of A-CNPS from anthocyanins and casein using sonication as a top-down technique.

Table 1 Optimization of anthocyanin quantity required to synthesize nanoparticles (NPs)

Sample	Anthocyanin (mg)	Size (nm)	PDI	Zeta potential (mV)
BP@A-CNPs	1	198.17 ± 1.18^{cd}	0.219 ± 0.009^{a}	-35.07 ± 1.01^{ad}
	3	228.97 ± 1.55^{b}	0.462 ± 0.003^{b}	-33.77 ± 1.30^{b}
	5	205.17 ± 3.10^{c}	0.461 ± 0.008^{ac}	-42.13 ± 1.36^{c}
	10	209.57 ± 1.08^{a}	0.360 ± 0.014^{a}	-39.73 ± 1.19^{a}
WB@A-CNPs	1	196.73 ± 1.18^{d}	0.187 ± 0.021^{bc}	-36.00 ± 1.04^{c}
	3	224.80 ± 4.81^{ab}	0.510 ± 0.045^{b}	-42.39 ± 1.28^{ab}
	5	234.03 ± 1.45^{c}	0.407 ± 0.003^{ab}	-35.33 ± 1.02^{ab}
	10	249.67 ± 1.35^{a}	0.392 ± 0.004^{a}	-39.10 ± 2.02^{a}
BB@A-CNPs	1	201.10 ± 0.88^{d}	0.241 ± 0.008^{cd}	-34.17 ± 0.94^{d}
	3	315.00 ± 4.10^{b}	0.450 ± 0.003^{b}	-36.63 ± 1.78^{b}
	5	209.60 ± 1.07^{c}	0.384 ± 0.004^{c}	-38.80 ± 2.15^{c}
	10	368.63 ± 5.96^{a}	0.420 ± 0.003^{a}	-32.83 ± 1.39^{a}

Data are expressed as mean ± standard deviation (n = 3). Mean values within the same sample and different concentrations with different superscripts (a–d) represent statistically significant differences ($p < 0.05$).

0.187–0.510, and 0.241–0.450, respectively. Consequently, these particles exhibit enhanced resistance against agglomeration and destabilization forces, including van der Waals forces, inter-particle interactions, and Brownian motion effects. In the case of BP@A-CNPs, WB@A-CNPs, and BB@A-CNPs, the zeta potential varies from −42.13 to −33.77, −42.39 to −35.33, and −38.80 to −32.83 mV, respectively.[26] As mentioned in ESI Fig. 2,† the zeta potential of bare CNPs was −33.0 mV, and the zeta potential of A-CNPs varied from −36.1 to −34.9 mV. Meanwhile, the size of bare CNPs was 184.7 nm, and the PDI was 0.124. Therefore, the casein to ACN (BP, WB, and BB) ratio of 100 : 1 was selected to synthesize A-CNPs for further studies based on their acceptable size, PDI, and zeta potential (Table 1).

3.2.1. Encapsulation efficiency of anthocyanin-casein-based nanonutraceuticals (A-CNPs). The BP, WB, and BB-based A-CNPs exhibited commendable encapsulation efficiency. The highest encapsulation efficiency (92.32%) was observed in the case of BB@A-CNPs, followed by BP@A-CNPs (83.18%). Meanwhile, WB@A-CNPs exhibited the least but acceptable encapsulation efficiency (72.41%), as mentioned in ESI Table 1.† Thus, it can be elucidated that BP, WB, and BB anthocyanins were effectively enclosed in CNPs. Previously, researchers have reported 45.4–96% encapsulation efficiency when they encapsulated anthocyanin in pectin and lysozyme self-assembly, maltodextrin and whey protein isolate, corn starch, amphiphilic peptide, β-lactoglobulin, and sodium caseinate-konjac glucomannan.[1,3,4,6,11,12]

The encapsulation efficiency of the resultant A-CNPs is influenced by the interaction between casein and ACNs. Additionally, the chemical composition of the ACN extract and its low concentration play a critical role in determining encapsulation efficiency. Given that different ACN types exhibit varying polarities and solubilities, their interactions with a specific wall material will be different depending on their source.[2] Furthermore, it is important to consider the degradation of anthocyanins already occurred before raw material collection and further processing from extraction to purification, as these also alter the functional groups responsible for interactions with casein, thereby impacting the encapsulation efficiency of A-CNPs.

Previous studies have identified malvidin 3-glucoside, delphinidin 3-glucoside, petunidin 3-glucoside, and cyanidin 3-galactoside as the predominant anthocyanins in BB.[27] In BP, the major anthocyanins were delphinidin-3-*O*-diglucoside, malvidin 3,5-*O*-diglucoside, petunidin 3-glucoside, and petunidin 3,5-*O*-diglucoside.[21] Conversely, black WB contains delphinidin-3-*O*-rutinoside, delphinidin-3-*O*-diglucoside, delphinidin-3-*O*-galactoside, and petunidin 3-glucoside as its primary anthocyanins.[28] Similarly, as shown in Table 2, the ACN composition of extracts from WB, BB, and BP was significantly different. Notably, the composition of individual anthocyanins may vary depending on factors such as cultivar type, geographical location, and the ripening or maturity stage of the plant material.[2] Consequently, variations in encapsulation efficiency observed in the present study may be attributed to significant differences in

Table 2 Composition of anthocyanins in black plum, blueberry, and wheat bran

S. no.	Anthocyanins	M/Z	MS/MS	BP	BB	WB
1	Cyanidin-3-glucoside	449	287, 449	+	−	−
2	Peonidin glucoside	463	301, 663	+	+	−
3	Delphinidin glucoside	465	303, 465	+	−	+
4	Malvidin-3-*O*-glucoside	493	331, 317, 493	+	+	+
5	Cyanidin succinyl glucoside	549	287, 549	+	+	+
6	Petunidin derivative	551	317, 551	−	+	+
7	Petunidin-*p*-coumaroyl glucoside	625	317, 625	+	+	−
8	Malvidin-3-rutinoside	639	317, 331	−	−	+
9	Malvidin-3,5-diglucoside	655	317, 655	−	+	+
10	Peonidin derivative	803	303, 413, 803	−	+	+
11	Malvidin	947	331, 947	+	+	+
12	Cyanidin rutinoside	595	287, 449, 595	+	+	+

both the composition and concentration of individual anthocyanins.

3.2.2. Characterization of A-CNPs. Furthermore, the particle size, PDI, and zeta potential of A-CNPs synthesized at an optimized casein : ACN ratio of 100 : 1 were observed using DLS. As shown in ESI Fig. 2,† bare CNPs had the smallest particle size of ~185 nm, PDI of 0.124, and zeta potential of −40 mV. Interestingly, the particle size of A-CNPs significantly increased, indicating successful encapsulation of ACNs inside casein.[17] Previously, the successful entrapment of gossypol within casein nanoparticles was also demonstrated based on the increase in particle size. Furthermore, the lower the polydispersity index (PDI) value, the better and more stable the dispersion of nanoparticles in solution.[12] The particle size of BP@A-CNPs was ~200 nm with 0.109 PDI and ~−35 mV surface charge. WB@A-CNPs exhibited a particle size, PDI, and zeta potential of ~195 nm, 0.173, and ~−36 mV, respectively. The low PDI value reflects the mono-dispersibility of the resultant A-CNPs.[17] Moreover, BB@A-CNPs exhibited a particle size of ~202 nm, a PDI of 0.242, and a zeta potential of −33 mV, respectively. Furthermore, the presence of a negative charge on the surface of A-CNPs results in repulsion between the resultant nanoparticles that contributes to their stability. All A-CNPs were of nanoscale size, demonstrating that the desolvation method in conjunction with the ultrasonication process constitutes an efficacious approach for the generation of protein-based anthocyanin nanoparticles.[3] The DLS data observed in the present study were in accord with previous studies focused on encapsulating anthocyanins using different kinds of wall materials.[3,4,6,11,12]

3.2.3. Morphological analysis of the synthesized A-CNPs. The morphological characterization of bare CNPs and A-CNPs was done using field emission-scanning electron microscopy (FE-SEM) at 500 nm (Fig. 1). The synthesized nanoparticles, including bare CNPs and A-CNPs, exhibited particle sizes of ~120–200 nm. Subsequently, the synthesized nanoparticles were polyhedral in shape with a rough surface. Convincingly, A-CNPs exhibited a noticeable increment in their particle size (~160 to ~200 nm) compared to bare CNPs (~120 to ~140 nm), indicating successful encapsulation of anthocyanins in casein. These results are in accordance with the observations of particle size distribution. Similar findings with an increase in particle size were also observed while nanoencapsulating red raspberry pomace anthocyanin in β-lactoglobulin. In addition, the shape of the resultant nanoparticles was also similar to polyhedral-shaped A-CNPs observed in the present study.[3] Previously, researchers have also reported the synthesis of ~210 nm resveratrol-loaded casein nanoparticles with a polyhedral shape and rough surface.[29]

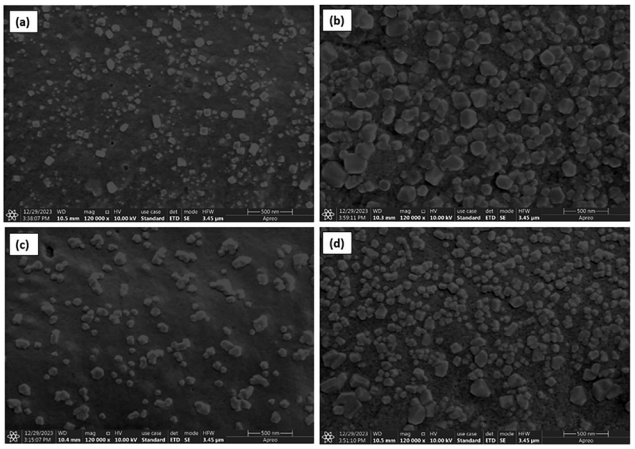

Fig. 1 SEM analysis of A-CNPs: (a) bare CNPs, (b) BP@A-CNPs, (c) WB@A-CNPs and (d) BB@A-CNPs.

3.2.4. Fourier-transform infrared (FTIR) spectroscopy. The FTIR spectrum of purified ACNs from BP, WB, and BB was acquired ranging from 400–4000 cm^{-1} (ESI Fig. 3†). The vibrational bands in the fingerprint region (600 to 1000 cm^{-1}) confirm aromatic rings, and the absorption band from 1500 to 2000 cm^{-1} corresponds to the benzene ring (C═C/C═N/C═O). The region from 3600 to 3200 cm^{-1} indicates H-bonds/O–H/N–H grouped, and the broad band from 3000 to 2800 cm^{-1} corresponds to C–H streching frequency. Thus, FTIR spectra of ACNs confirm the presence of characteristic functional groups (O–H, C═O, C═C, and C–O–C) of ACNs.[30] The absorbance band at 1246 cm^{-1} and 1018 cm^{-1} represents the stretching of pyran rings and the stretching vibration of C–O–C esters, respectively. The absorbance bands at 1707, 1647, and 1423 cm^{-1} correspond to the C═O and C═C groups of aromatic rings and C–O deformation of phenols, respectively. The band at 1600 cm^{-1} corresponds to the skeletal stretching vibration of aromatic rings (A and B) of ACNs and ═C–O–C of flavones (C ring). The bands at 1514, 1462, 1246, and 1018 cm^{-1} represent the stretching vibration of the ═C–O–C group in the aromatic ring of flavonoids. The bands at 804 and 742 cm^{-1} correspond to the vibration of anthocyanins.[31] Additionally, the FTIR spectrum of casein was also recorded. Notably, the amide A and amide B bands were observed at 3455 and 3100 cm^{-1} due to Fermi resonance between the first overtone of amide II and N–H stretching vibrations. An intense band at around 1661 cm^{-1} for amide I was observed due to the C═O stretching vibration related to backbone conformation and hydrogen bonding. The amide II bands were observed at 1510 and 1580 cm^{-1}, representing the N–H bending vibration and C–N stretching vibration. The bands at 1661 and 1531 cm^{-1} confirm the alpha-helical structure of casein. Another characteristic band at 1415 cm^{-1} corresponds to the carboxylate group (O–C–O) present in casein.[32] Interestingly, FTIR spectra of BP@A-CNPs, WB@A-CNPs, and BB@A-CNPs displayed characteristic peaks of purified anthocyanins and casein, confirming the synthesis of A-CNPs.

3.2.5. HPLC analysis. The HPLC analysis of A-CNPs was carried out to determine the amount of anthocyanin encapsulated in casein nanoparticles.[30] Therefore, HPLC analysis of standard anthocyanins delphinidin and petunidin was performed. Furthermore, the HPLC analysis of A-CNPs (BP@A-CNPs, WB@A-CNPs, and BB@A-CNPs) was conducted. The significant standard peaks of anthocyanin were observed

in A-CNPs, confirming anthocyanin's encapsulation in casein nanoparticles (ESI Fig. 4†).

3.3. Stability study of anthocyanin-encapsulated casein nanonutraceuticals (A-CNPs)

3.3.1. Storage stability of A-CNPs at room temperature based on DLS data. The potential application of A-CNPs is the fortification of flavored water and ultra-high-treated beverages. These products are transported and stored at room temperature during retailing. Thus, the storage stability of bare CNPs, BP@A-CNPs, WB@A-CNPs, and BB@A-CNPs was investigated at room temperature for 28 days under natural light with 16 h of daily light exposure based on DLS data. As shown in ESI Fig. 5,† insignificant variations were observed in the particle size, PDI, and zeta potential during storage. Thus, the synthesized A-CNPs were stable for a long time at room temperature with no aggregation. This observation confirms the efficient application of the synthesized A-CNPs for long-term use as additives in fortified beverages or foods. In a previous study, researchers have also reported the protective effects of casein on BB anthocyanin towards light, temperature, and pH change. It was mentioned that encapsulation of BB ACNs by casein through van der Waals forces and hydrogen bonding enhances the stability of ACNs.[33]

3.3.2. Stability of A-CNPs towards temperature, pH, and light. It is well known that purified anthocyanin exhibits poor stability towards high temperature, pH variation, and light, which hinders the successful application of anthocyanins as additives in food.[2] Therefore, the thermal stability of the synthesized A-CNPs in terms of percentage ACN retention rate was investigated while heating at 80 °C for 5 h at an interval of 1 h. As observed in Fig. 2(a and b), the hourly retention rate of ACNs (BP, WR, and BB) was significantly reduced with increased thermal treatment time. Meanwhile, the ACN retention rate of A-CNPs was comparatively higher than that of the purified ACNs. It is important to note that BB@ACNs (Fig. 2c) exhibited the highest hourly retention rates (98.50–83.22%) compared to WB@A-CNPs (98.08–75.28%), as shown in Fig. 2b. Meanwhile, BP@A-CNPs exhibited satisfactory but the lowest ACN retention rates (97.91–62.54%), as shown in Fig. 2a. ESI Fig. 5 and 6† show vials containing purified ACNs and A-CNPs from BP, WB, and BB heated at 80 °C for different time intervals, respectively. Previously, raspberry ACN nanoencapsulated using β-lactoglobulin and BB ACNs encapsulated with α- and β-casein exhibited improved thermal stability.[3,33]

Furthermore, purified ACNs and A-CNPs from BP, WB, and BB were exposed to light for 16 h for 28 days at room temperature. A significant visual change in the color of purified ACNs represents gradual degradation during the 28 days (ESI Fig. 8†). Meanwhile, the least color variation was observed in A-CNPs when exposed to light for 28 days (ESI Fig. 9†). In terms of ACN retention rate, purified ACNs showed a significant decrease with an increase in light exposure time (Fig. 2d–f). ACNs from BP exhibited the most prominent decrease in the ACN retention rate (Fig. 2d) compared to WB (Fig. 2e) and BB ACNs (Fig. 2f). After nanoencapsulation, significant

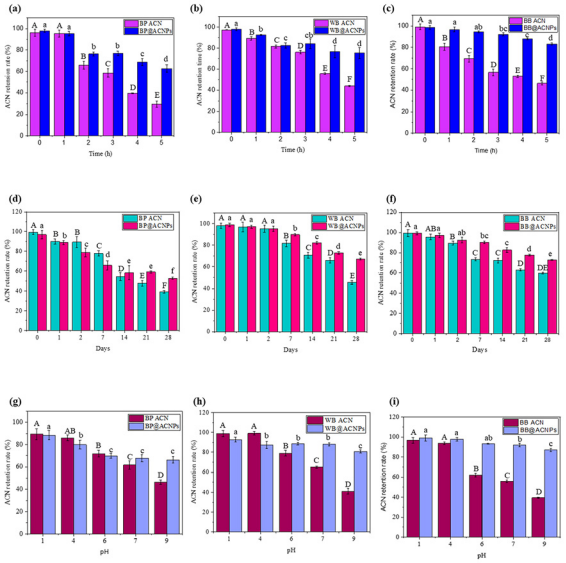

Fig. 2 Anthocyanin retention rates of purified anthocyanins from BP, WB, BB and BP@A-CNPs, WB@A-CNPs, BB@A-CNPs in response to (a–c) thermal treatment at 80 °C, (d–e) natural light for 28 days, and (g–i) different pH values. Data were expressed as mean ± standard deviation (n = 3). Data bars with different superscripts (A–E) and (a–e) represent statistically significant differences among ACNs and A-CNPs, respectively ($p < 0.05$).

improvement in ACN retention rates of A-CNPs was observed. BB@A-CNPs exhibited the highest stability (99.03–72.84%) towards 28 days of light exposure (Fig. 2f) compared to BP@A-CNPs (96.97–52.68%) and WB@@A-CNPs (98.89–67.14%), as shown in Fig. 2(d and e). Similar results were also observed in a previous study, where mulberry ACNs nanoencapsulated with sodium caseinate-konjac glucomannan exhibited higher stability towards light compared to bare ACNs. This increased stability was attributed to the formation of H-bonding between ACNs and casein that significantly enhanced the stability of the core wall structure.[12]

Furthermore, stability across different pH ranges is another key parameter for evaluating the stability of nanocomplexes, confirming that the resultant nanoparticles were effective in maintaining colloidal stability. As observed in ESI Fig. 10,† pH has a significant impact on ACNs collected from BP, WB, and BB. However, a change in pH has an insignificant visual impact on A-CNPs, as shown in ESI Fig. 11.† In terms of ACN retention rate, the change in ACN (BP, WB, and BB) pH from 1 to 9 significantly reduces the ACN retention rate (Fig. 2g–i). In the case of A-CNPs, the highest retention rate was observed in BB@A-CNPs (98.96–86.88%), as shown in Fig. 2(i), followed by 92.67–80.71% in WB@A-CNPs (Fig. 2h) and the least retention rate was observed in the case of BP@A-CNPs (88.43–66.32%), as observed in Fig. 2(g). Moreover, the stability of A-CNPs may be attributed to the electrostatic interaction between the cationic regions of anthocyanins and the anionic groups of casein.[6] Thus, nanoencapsulation of ACNs could prevent their interaction with other food components, which is a critical

factor for enhancing the chemical stability of these bioactive compounds during food storage, particularly in the development of new food additives.[34] Based on the observations of stability studies (Fig. 2), BB@A-CNPs exhibit the highest stability towards pH change, temperature, and light. Previously, nanoencapsulation of ACNs with amphiphilic peptides and sodium caseinate-konjac glucomannan also exhibited improved stability towards pH changes.[1,12]

3.4. Gastrointestinal digestion of BB@A-CNPs

Based on the findings of the stability study, BB@A-CNPs can be used as an additive for developing functional foods rich in anthocyanins. Anthocyanins exhibit relatively high stability during simulated gastric digestion. However, the alkaline environment of intestinal juice is the primary factor leading to their degradation and reduced accessibility. Consequently, protective measures for anthocyanins should be concentrated on the intestinal digestion phase.[33] Thus, it is crucial to explore the fate of BB@A-CNPs under *in vitro* gastrointestinal digestion and compare it with purified BB ACNs. The results of *in vitro* gastrointestinal digestion of purified BB ACNs and BB@A-CNPs are shown in Fig. 3(a). During oral digestion, the residence time for both BB ACNs and BB@A-CNPs was less in the mouth, and thus, negligible degradation was observed.

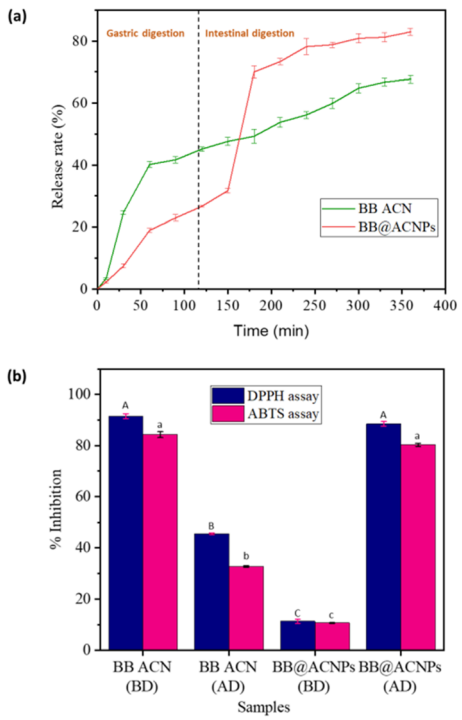

Fig. 3 (a) Gastrointestinal digestion of purified BB ACN and BB@A-CNPs, (b) antioxidant potential of purified BB ACN and BB@A-CNPs before gastrointestinal digestion (BD) and after gastrointestinal digestion (AD). Data were expressed as mean ± standard deviation (n = 3). Data bars with different superscripts (A–C) and (a–c) represent statistically significant differences among DPPH and ABTS values, respectively ($p < 0.05$).

During gastric digestion, a significant release of BB ACNs was observed (Fig. 3a). In the case of BB@A-CNPs, the least ACN release was also observed with an increase in digestion time. This may be attributed to the least decomposition of macromolecular proteins and the weakening of crosslinking by $CaCl_2$. It was mentioned that pepsin attacks peptide bonds containing hydrophobic aromatic amino acids. In the case of BB@A-CNPs, the majority of these amino acids, due to their hydrophobicity, might be trapped inside the protein network during the synthesis of A-CNPs by the addition of $CaCl_2$.[35] At the end of the gastric digestion, there was a significant difference in the release rate of BB ACNs (25.35%) and BB@A-CNPs (48.41%), indicating that casein as a wall material and $CaCl_2$ as a crosslinking agent delayed the release of ACNs in the environment. During this phase, an acidic environment induces degradation of ACNs, which continue to reconvert into ACNs until they reach the next phase.[36] Overall, BB@A-CNPs remain relatively stable in gastric juices and show slower release than BB ACNs. BB@A-CNPs continue to release slowly during the initial intestinal digestion. Similar observations were also reported in previous studies on nanoencapsulated anthocyanins.[12,37] After alkaline intestinal digestion, the release rate of BB@A-CNPs significantly increased compared to BB ACNs. It was mentioned that the polyhydroxyl structure of ACNs is responsible for their poor stability under alkaline environments, and pancreatic enzymes in intestinal fluid further break down casein and $CaCl_2$-based wall materials.[35,38]

Furthermore, the antioxidant potential of the final digesta of both BB ACNs and BB@A-CNPs was also explored by employing the DPPH and ABTS assays. As shown in Fig. 3b, purified BB ACNs exhibit significantly higher antioxidant activity before digestion; however, a substantial decrease in their antioxidant potential was observed after *in vitro* gastrointestinal digestion. Meanwhile, BB@A-CNPs exhibit poor antioxidant activity before digestion, as ACNs were encapsulated inside casein nanoparticles. At the end of the digestion experiment, a significant increase in the antioxidant activity was observed, indicating the release of anthocyanins in the intestine due to the action of pancreatic enzymes. These observations were in accord with a previous study on the gastrointestinal fate of BB ACNs encapsulated using ferritin nanocarriers.[39] Based on these observations, BB@A-CNPs with enhanced stability and improved gastrointestinal digestion can be a promising additive for developing novel functional foods and nutraceuticals.

4. Conclusion

The present study successfully demonstrated the extraction of anthocyanins from secondary-agricultural residues and their subsequent nanoencapsulation using casein as a wall material. The nanoencapsulation process not only improved the stability of anthocyanins against environmental stressors such as temperature, pH, and light but also enhanced their bioavailability, as evidenced by the *in vitro* gastrointestinal digestion model.

The high encapsulation efficiency and improved physicochemical stability of A-CNPs, particularly BB@A-CNPs, make them a promising candidate for functional food additives. BB@A-CNPs also presented improved bioavailability under *in vitro* gastrointestinal digestion. Thus, these A-CNPs, particularly BB@A-CNPs, could potentially be integrated into dairy products or other food systems to boost their nutritional value and health benefits. Future research should be focused on scaling up the production process and conducting *in vivo* studies to further validate the health claims associated with consuming these anthocyanin-based nanonutraceuticals. The findings of the present study contribute to the circular economy by repurposing food waste and highlighting the potential of nanoencapsulation in improving the utility and applicability of bioactive compounds in the food industry.

Author contributions

Maninder Meenu: conceptualization, data curation, methodology, investigation, writing – original draft, and visualization. Mansi: investigation, methodology, and writing – review & editing. Anil Kumar Pujari: methodology and writing – review & editing. Monika Garg: methodology and writing – review & editing. Jayeeta Bhaumik: conceptualization, investigation, supervision, project administration, and writing – review & editing.

Data availability

The data supporting this article have been included as part of the ESI.†

Conflicts of interest

The authors declare that they have no known competing financial interests or personal relationships that could have appeared to influence the work reported in this paper.

Acknowledgements

The authors would like to acknowledge the Department of Biotechnology (DBT), Govt. of India, for funding and infrastructural support. This work is supported by the M. K. Bhan Young Researcher Fellowship, Department of Biotechnology, New Delhi, India to M. M. J. B. thanks DBT for funding under lignin valorization flagship project. The authors would also like to acknowledge NABI and CIAB Mohali for providing the instrumentation facilities.

References

1 L. Yao, J. Xu, L. Zhang, L. Liu and L. Zhang, *Food Hydrocolloids*, 2021, **118**, 106741.
2 M. Meenu, V. Bansal, S. Rana, N. Sharma, V. Kumar, V. Arora and M. Garg, *Sustainable Chem. Pharm.*, 2023, **34**, 101168.
3 M. Salah, M. Mansour, D. Zogona and X. Xu, *Food Res. Int.*, 2020, **137**, 109635.
4 R. Rashid, S. M. Wani, S. Manzoor, F. A. Masoodi and A. Altaf, *Food Biosci.*, 2022, **50**, 102135.
5 M. Meenu, A. K. Pujari, S. Kirar, M. Mansi, A. Thakur, M. Garg and J. Bhaumik, Development of bionanocomposite packaging film based on lignin nanoencapsulated anthocyanins extracted from agro-waste for enhancing post-harvest shelf life of tomatoes, *Sustainable Food Technol.*, 2025, **3**, 414–424.
6 T. K. O. Rosales, M. P. da Silva, F. R. Lourenço, N. M. A. Hassimotto and J. P. Fabi, *Food Hydrocolloids*, 2021, **114**, 106563.
7 S. Kirar, D. Mohne, M. Singh, V. Sagar, A. Bhise, S. Goswami and J. Bhaumik, *Sustainable Mater. Technol.*, 2024, **40**, e00864.
8 Z. Fu, H. Ju, G. S. Xu, Y. C. Wu, X. Chen and H. J. Li, *Food Chem.*, 2024, **439**, 138104.
9 S. Paul, N. S. Thakur, S. Chandna, Y. N. Reddy and J. Bhaumik, *J. Mater. Chem. B*, 2021, **9**, 1592–1603.
10 R. Kaur, N. S. Thakur, S. Chandna and J. Bhaumik, *ACS Sustainable Chem. Eng.*, 2021, **9**, 11223–11237.
11 A. A. Escobar-Puentes, A. García-Gurrola, S. Rincón, A. Zepeda and F. Martínez-Bustos, *Carbohydr. Polym.*, 2020, **250**, 116972.
12 H. Zhang, C. Jia, Y. Xiao, J. Zhang, J. Yu, X. Li, N. Hamid and A. Sun, *Food Chem.*, 2024, **439**, 138150.
13 U. Ali, E. Chaudhary, S. Kaur, A. Sharma, M. Yadav, A. Kumari, B. Sheoran, V. Tiwari, S. Sharma, A. Tiwari and M. Garg, *J. Cereal Sci.*, 2023, **113**, 103757.
14 U. Ali, A. Kumari, A. Sharma, M. Yadav, S. Kaur, E. Chaudhary, B. Sheoran, V. Tiwari, A. Tiwari, P. Singh, R. Nain, A. Goyal and M. Garg, *J. Cereal Sci.*, 2024, **118**, 103957.
15 L. Zheng, L. Liu, J. Yu, M. A. Farag and P. Shao, *Food Control*, 2023, **151**, 109798.
16 A. Kumari, S. Kaur, N. Sharma, J. Kaur, M. Krishania, V. Tiwari and M. Garg, *J. Cereal Sci.*, 2022, **108**, 103560.
17 G. B. Patil, D. M. Borse, M. P. More and D. A. Patil, *J. Pharm. Innov.*, 2023, **18**, 563–574.
18 M. S. Lingua, D. A. Wunderlin and M. V. Baroni, *J. Funct. Foods*, 2018, **44**, 86–94.
19 M. Ahmad, B. Ashraf, A. Gani and A. Gani, *Int. J. Biol. Macromol.*, 2018, **109**, 435–442.
20 W. Yang, Y. Guo, M. Liu, X. Chen, X. Xiao, S. Wang, P. Gong, Y. Ma and F. Chen, *J. Funct. Foods*, 2022, **88**, 104864.
21 N. R. R. do Nascimento-Silva, R. P. Bastos and F. A. da Silva, *J. Food Compos. Anal.*, 2022, **109**, 104491.
22 Z. Wu, M. Meenu and B. Xu, *LWT–Food Sci. Technol.*, 2021, **135**, 110226.
23 N. Solarte, M. J. Cejudo-Bastante, N. Hurtado and F. J. Heredia, *Int. J. Food Sci. Technol.*, 2022, **57**, 2416–2423.

24 W. Liao, W. Badri, E. Dumas, S. Ghnimi, A. Elaissari, R. Saurel and A. Gharsallaoui, *Appl. Sci.*, 2021, **11**, 5778.
25 R. Esfahani, S. M. Jafari, A. Jafarpour and D. Dehnad, *Food Hydrocolloids*, 2019, **90**, 291–298.
26 M. A. Çakır, N. C. Icyer and F. Tornuk, *Int. J. Biol. Macromol.*, 2020, **151**, 230–238.
27 D. D. Herrera-Balandrano, Z. Chai, T. Beta, J. Feng and W. Huang, *Trends Food Sci. Technol.*, 2021, **118**, 808–821.
28 S. Sharma, A. Kumar, D. Singh, A. Kumari, P. Kapoor, S. Kaur, B. Shreon and M. Garg, *Plant Physiol. Biochem.*, 2022, **189**, 59–70.
29 R. Peñalva, J. Morales, C. J. González-Navarro, E. Larrañeta, G. Quincoces, I. Peñuelas and J. M. Irache, *Int. J. Mol. Sci.*, 2018, **19**, 2816.
30 B. Bhushan, B. Bibwe, A. Pal, M. K. Mahawar, M. C. Dagla, Y. Kr, P. Kumar, S. K. Aggarwal, A. Singh and D. P. Chaudhary, *Appl. Food Res.*, 2023, **3**, 100282.
31 R. Różyło, M. Szymańska-Chargot, U. Gawlik-Dziki and D. Dziki, *Food Chem.*, 2021, **346**, 128889.
32 A. Singh, J. Bajpai, A. Tiwari and A. K. Bajpai, *Prog. Biomater.*, 2015, **4**, 39–53.
33 Y. Lang, H. Gao, J. Tian, C. Shu, R. Sun, B. Li and X. Meng, *LWT–Food Sci. Technol.*, 2019, **115**, 108434.
34 S. Ghasemi, S. M. Jafari, E. Assadpour and M. Khomeiri, *Food Hydrocolloids*, 2018, **77**, 152–162.
35 R. Penalva, I. Esparza, M. Agüeros, C. J. Gonzalez-Navarro, C. Gonzalez-Ferrero and J. M. Irache, *Food Hydrocolloids*, 2015, **44**, 399–406.
36 R. N. Cavalcanti, D. T. Santos and M. A. A. Meireles, *Food Res. Int.*, 2011, **44**, 499–509.
37 X. Zhao, X. Zhang, S. Tie, S. Hou, H. Wang, Y. Song, R. Rai and M. Tan, *Food Hydrocolloids*, 2020, **109**, 106114.
38 B. Enaru, G. Drețcanu, T. D. Pop, A. Stănilă and Z. Diaconeasa, *Antioxidants*, 2021, **10**, 1967.
39 D. D. Herrera-Balandrano, Z. Chai, L. Cui, X. Zhao, X. Zhao, B. Li, Y. Yang and W. Huang, *Food Res. Int.*, 2024, **176**, 113811.